

Ozone and Aerosol Optical Depth Retrievals Using the Ultraviolet Multi-Filter Rotating Shadow-band Radiometer

Joseph Michalsky¹ and Glen McConville^{1,2}

¹Global Monitoring Laboratory, National Oceanic and Atmospheric Administration,
325 Broadway, Boulder, Colorado 80305 USA

²Cooperative Institute for Research in Environmental Sciences, University of Colorado,
216 UCB, Boulder, Colorado 80309 USA

Correspondence to: Joseph Michalsky (joseph.michalsky@noaa.gov)

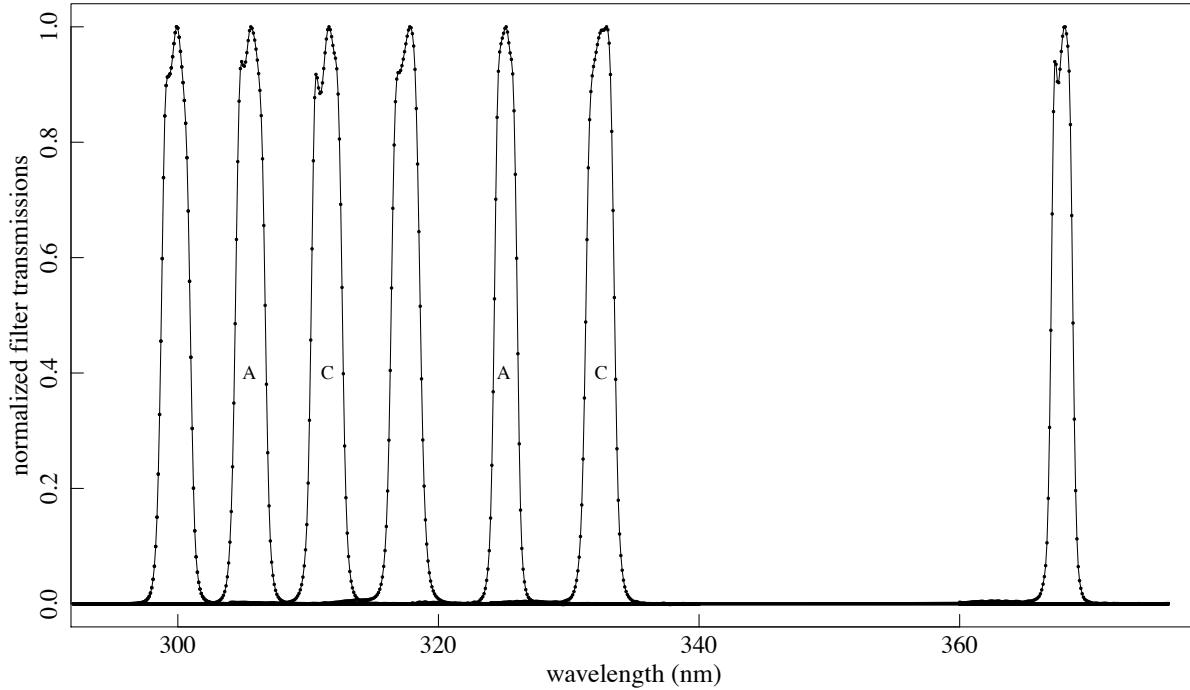
Abstract: The ultraviolet multi-filter rotating shadowband radiometer (UV-MFRSR) is a seven-channel radiometer with narrowband filters centered between wavelengths 300 and 368 nm. Four of the middle wavelengths in this device are near those used in the Dobson spectrometer to retrieve ozone column abundance. In this paper measurements from Mauna Loa Observatory (MLO) were used, first, to calibrate the instrument using the Langley plot method, and, subsequently, to derive column ozone and aerosol optical depths. The ozone derived from the UV-MFRSR was compared to the ozone measured by a Dobson spectrophotometer that operates daily at the MLO resulting in column values within about 1 DU on average for 43 days in 2018. The aerosol optical depth (AOD) retrievals are more challenging. Generally, the AOD increases with wavelength between 305 and 332 nm; not what is expected given the typical AOD wavelength dependence at visible wavelengths. An example of this behavior is discussed, and research by others is cited that indicates similar behavior at these wavelengths, at least for the low aerosol optical depth conditions encountered at high altitude sites.

Ozone Retrieval Introduction

Most historical network measurements of column ozone from the surface used Dobson or Brewer spectrometers, and these continue as the predominant ozone measurement instruments today. Brief explanations of these two devices and comparisons of concurrent and collocated measurements of total column ozone are given in Staehelin et al. (2003). Gao et al. (2001) demonstrated that ozone could be retrieved using the ultraviolet multi-filter rotating shadow-band radiometer (UV-MFRSR), which agreed with those values retrieved from either collocated Dobson and/or Brewer spectrophotometers to within 1-2%.

The wavelengths used for ozone retrievals in the UV-MFRSR more closely match wavelengths in the Dobson rather than the Brewer spectrophotometer. Typically, ozone retrieved from the Dobson uses the AD wavelength pairs 'A' 305.5/325.4 and 'D' 317.6/339.8. Since there is no filter near 339.8 nm, the UV-MFRSR uses filters near the 'A' pair and the Dobson 'C' pair 311.5/332.4. The filters in the UV-MFRSR that are used for ozone measurements are nominally the 305/325 nm pair and the 311/332 nm pair with carefully measured profiles of these filters used for actual retrievals. Normalized filter profiles for UV-MFRSR 453 are shown in Figure 1.

Filter Profiles for UV-MFRSR 453



46 **Figure 1. Normalized filter profiles of UV-MFRSR 453 used in this study. The wavelength-dependent ozone**
 47 **absorption function and Rayleigh scattering function were convolved with these profiles to produce effective**
 48 **absorption and scattering corrections. ‘A’ and ‘C’ pairs used for ozone retrievals are noted. Central**
 49 **wavelength/full width at half maximum (nm): 299.9/2.2, 305.6/2.3, 311.4/2.4, 317.5/2.3, 325.1/1.8, 332.4/2.2,**
 50 **367.8/1.7.**
 51

52
 53 The basic procedure for ozone retrievals consists of measuring extinction at two wavelengths
 54 with one chosen to be more strongly attenuated than the other in the Hartley-Huggins ultraviolet
 55 bands. The basic extinction equation can be written
 56

$$I(\lambda) = I_0(\lambda) \cdot \exp \left[-\tau_{ray}(\lambda)m_{ray}(\lambda) \left(\frac{P}{P_0} \right) - \tau_{oz}(\lambda)m_{oz}(\lambda) - \tau_{aer}(\lambda)m_{aer}(\lambda) \right] \quad (1)$$

57
 58 or, equivalently,
 59

$$V(\lambda) = V_0(\lambda) \cdot \exp \left[-\tau_{ray}(\lambda)m_{ray}(\lambda) \left(\frac{P}{P_0} \right) - \tau_{oz}(\lambda)m_{oz}(\lambda) - \tau_{aer}(\lambda)m_{aer}(\lambda) \right] \quad (2)$$

60 since the ratios I/I_0 and V/V_0 are equal.
 61

In these equations:

- $I(\lambda)$ = spectral irradiance measured by the instrument at the surface
- $I_0(\lambda)$ = spectral irradiance measured by the instrument at the top of the atmosphere
- $V(\lambda)$ = signal (voltage) measured by the instrument at the surface

$V_0(\lambda)$ = signal (voltage) measured by the instrument at the top of the atmosphere
 τ 's = optical depths for Rayleigh scattering (ray), ozone (oz), and aerosol (aer)
 P, P_o = atmospheric pressure at the measurement site and at sea level, respectively
 m 's = airmasses for Rayleigh, ozone, and aerosol relative to a vertical path; they differ slightly because each has a different distribution with altitude in the atmosphere. The Rayleigh and ozone air masses were calculated using Bodhaine et al., (1999) and Komhyr and Evans (2008), respectively.

62 If we write ozone optical depth as $\tau_{oz} = \alpha_{oz} \cdot \eta_{oz}$, where α_{oz} is the ozone absorption coefficient
 63 and η_{oz} is the abundance of ozone, we can solve for η_{oz} by rearranging terms in two versions of
 64 eqn. (2) representing the two wavelengths in the pair (the longer wavelength is indicated by
 65 primes). Therefore, dropping the explicit λ dependence for clarity, we get for ozone abundance
 66

$$\eta_{oz} = \frac{N - (\tau_{ray} - \tau'_{ray})m_{ray}(P/P_o) - (\tau_{aer} - \tau'_{aer})m_{aer}}{(\alpha_{oz} - \alpha'_{oz})m_{oz}}, \quad (3)$$

67
 68
 69 where N is defined as

$$N = \ln(V_o/V'_o) - \ln(V/V').$$

71
 72 Since all of the parameters of eqn. (3) are known or can be calculated, one could solve for η_{oz} if
 73 the term $(\tau_{aer} - \tau'_{aer})$, i.e., the aerosol optical depths at the two wavelengths were known. To
 74 curtail this requirement, the 'A' and 'C' wavelength pairs are used, and the assumption is made
 75 that since the wavelength separation of each pair is nearly the same and the wavelength
 76 dependence over this small wavelength region is expected to be nearly linear, subtraction of eqn.
 77 (3) applied to each pair will come very close to eliminating the aerosol terms because subtraction
 78 of aerosol terms should be near zero if these assumptions hold. The resulting equation used to
 79 calculate ozone is
 80

$$\eta_{oz} = \frac{N_1 - N_2 - [(\tau_{ray} - \tau'_{ray})_1 - (\tau_{ray} - \tau'_{ray})_2]m_{ray}(P/P_o)}{[(\alpha_{oz} - \alpha'_{oz})_1 - (\alpha_{oz} - \alpha'_{oz})_2]m_{oz}}, \quad (4)$$

81
 82
 83 where

$$N_1 = \ln(V_{o,305}/V'_{o,325}) - \ln(V_{305}/V'_{325}),$$

84
 85
 86 and

$$N_2 = \ln(V_{o,311}/V'_{o,332}) - \ln(V_{311}/V'_{332}).$$

89

90
91
92
93
94
95
96
97
98
99
100
101
102
103
104
105
106
107
108
109
110
111
112
113
114
115
116
117
118
119
120
121
122

Calibration and Ozone Measurement Comparisons

The Langley calibration of the UV-MFRSR was performed at NOAA's Mauna Loa Observatory (Latitude = 19.5362°N; Longitude = 155.5763°W; 3397 m). The height of the observatory often allows measurements to be made in clean, free-tropospheric air above the marine boundary layer, especially in the morning hours.

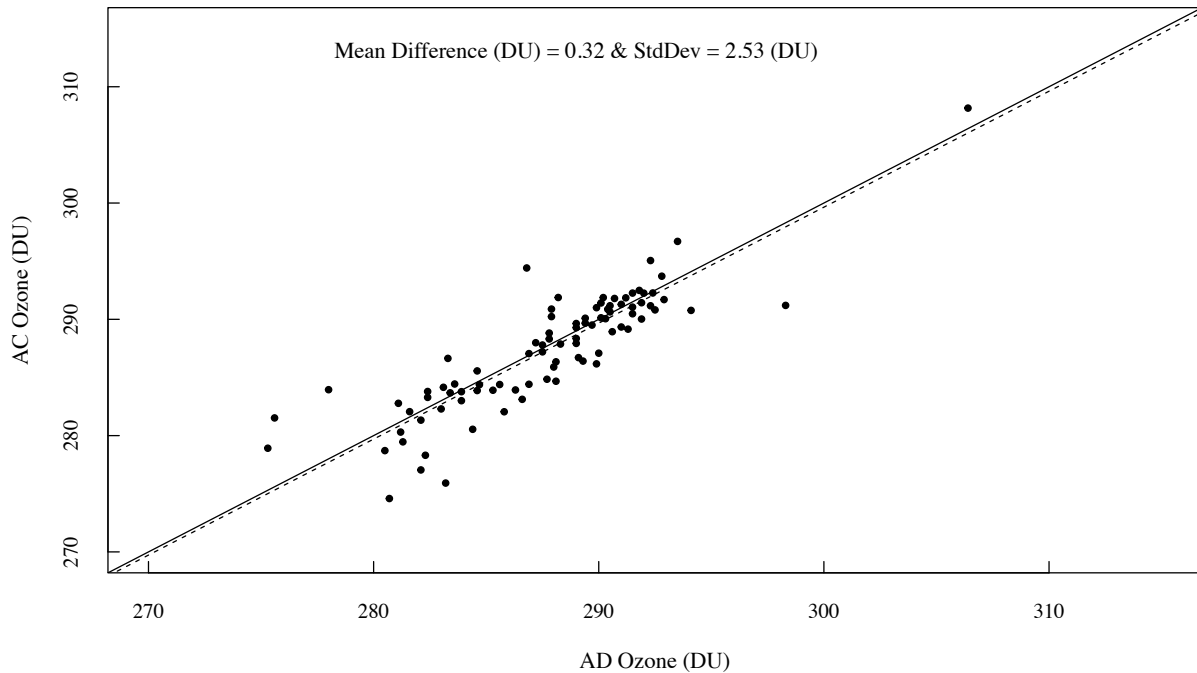
UV-MFRSR data were obtained on 242 days in 2018 beginning on 14 February and ending on 15 October. There were 139 successful Langleys during this period that produced estimated V_o 's with only 27 of these during the afternoon hours. Looking at the retrieved V_o 's as a function of time there is a hint of a decrease, but not one filter indicates a statistically significant decline, therefore, averages of V_o 's over the entire period are used in the ozone and aerosol retrievals.

The process used to choose acceptable Langleys (Michalsky et al., 2001) eliminates Langleys that are influenced by large changes in ozone during a Langley plot. Further, rarely did the standard deviation of the ozone sampled change by more than 5 DU during a morning or afternoon when Langley plots are sampled. This small change is typical for this low latitude.

Ozone is a standard measurement at NOAA's Mauna Loa Observatory and has been made with near continuous sampling since 1963. The Dobson spectrophotometer there makes AD paired measurements to determine ozone using absorption coefficients measured by Bass and Paur (1985). No estimate of the ozone column below the observatory, which could be on the order of 5% of the column total at sea level, is made. Therefore, the column measurements made using the UV-MFRSR can be directly compared to the Dobson column measurements if one uses the Bass and Paur (1985) absorption cross-sections for the UV-MFRSR channels.

Since the Dobson generally uses the AD pair for the total column ozone calculation, we investigated the difference between AC and AD Dobson retrievals on two clear days at Mauna Loa that were used for Langley calibrations of the Dobson thus giving us more than the operational 1000, 1200, and 1400 local time ozone measurements. It is important to assess any differences since the UV-MFRSR uses wavelengths close to the AC pair for its ozone retrievals. Figure 2 illustrates the difference between Dobson measurements with the two different

Ozone at MLO Using AC vs AD Pair



123
124
125
126
127
128

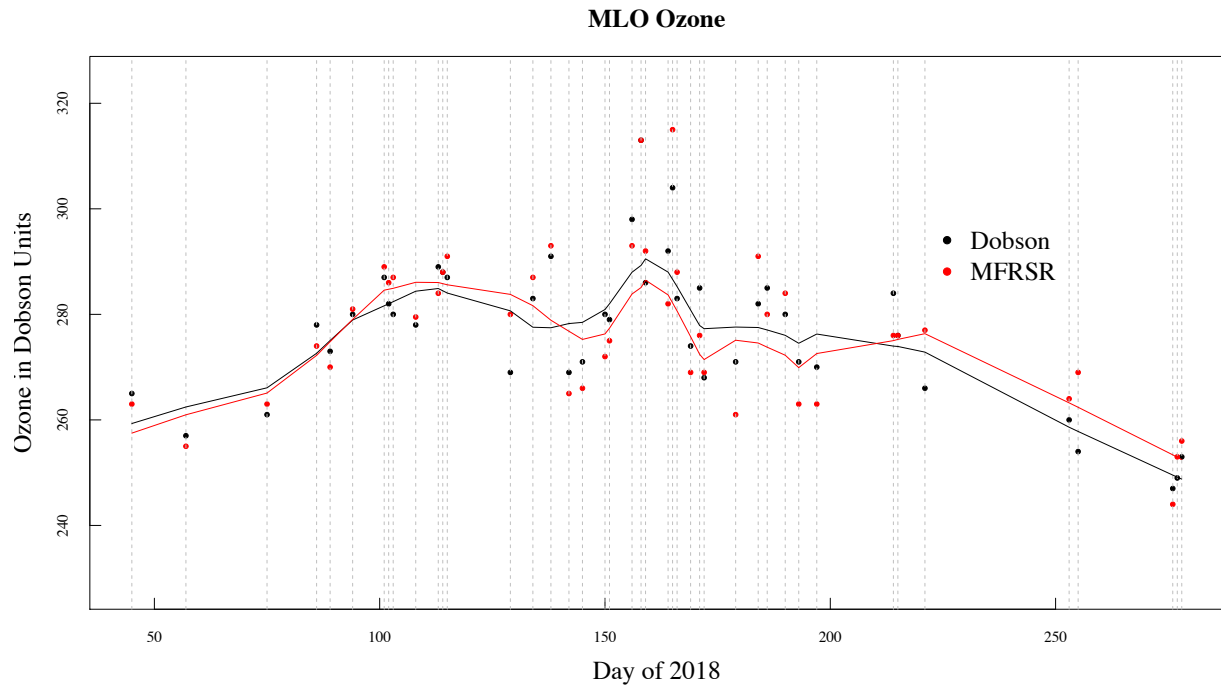
Figure 2. Plot of ozone measured by a Dobson unit at Mauna Loa Observatory retrieved using the Dobson AC pair versus the Dobson AD pair. Solid diagonal line is 1:1 line and dashed line is linear least-squares fit. The mean difference and standard deviation of the samples are given on the plot.

129 wavelength pairs. The mean difference in retrieved ozone for the 90 points compared in the plot
130 is less than 0.5 DU and the standard deviation among the 90 samples is close to 2.5 DU.
131 Therefore, using the AC pair of the UV-MFRSR for ozone retrievals and comparing to AD-pair
132 Dobson ozone should be acceptable.

133

134 Figure 3 is a plot of the ozone time series retrieved from the Dobson AD pair and the UV-
135 MFRSR AC pair for the 2018 data that were matched by day of year. In the case of the Dobson,

136 one measurement is chosen from the three daily measurements made at 1000, 1200 and 1400



137
138 **Figure 3. Time series plot of Mauna Loa Observatory for 43 days of retrieved ozone for 2018 using the**
139 **Dobson spectrophotometer (black dots) and the UV-MFRSR (red dots). The lines are lowess fits using 0.25 of**
140 **the points for the lowess fit at each point. The Dobson uses one of three measured points for the daily value,**
141 **and the UV-MFRSR uses the median of all 20-second, clear-sun data for air masses less than three.**

142
143
144 local standard time. Only direct sun measurements made with the Dobson are used for this
145 comparison. For the UV-MFRSR data, which is sampled every 20 seconds, a median value of all
146 points, which are made at less than three air masses and that pass cloud-screening (Michalsky et
147 al., 2010), is used. Since measurements from the two instruments are made differently and no
148 attempt to make them coincident, except for occurring on the same day, there is no expectation
149 of perfect agreement given any diurnal variability. The average difference over the 43-day
150 sample is about 0.10 Dobson units. The lowess fits to the two data sets track each other rather
151 closely matching dips and peaks throughout the measurement period.

152
153
154 **Sources of Ozone Uncertainty**

155
156 Uncertainties in using a UV-MFRSR for ozone retrievals were discussed thoroughly by Gao et
157 al. (2001). In this paper only data taken at less than three air masses (about 71° solar-zenith
158 angle) were used because (1) air mass determination is less certain at higher solar-zenith angles
159 and the cosine response correction for the UV-MFRSR is larger and more difficult to pinpoint
160 and, therefore, more uncertain. The extraterrestrial responses for the four filters used to retrieve
161 ozone were averages for the 242-day period in 2018 as stated earlier. The uncertainties in
162 extraterrestrial responses were between 0.2% and 0.3%. The ozone absorption coefficients were
163 those measured by Bass and Paur (1985) adjusted for mid-latitude seasonal variations. The
164 effective ozone absorption coefficients were determined by convolving each of the filter profiles

165 with the wavelength dependent Bass and Paur (1985) ozone absorption coefficients. Similarly,
166 effective Rayleigh scattering optical depths were determined in the same manner. The effective
167 Rayleigh optical depths were pressure corrected using on-site measurements of atmospheric
168 pressure.

169
170 Always a major concern when working in the ultraviolet is light from outside the band passes
171 contributing to the measured signal. Si-C (silicon carbide) is the detector for the 300 nm and 305
172 nm filters. GaP (gallium phosphide) is used as the detector in the five longest wavelength filters.
173 To measure the extent of the possible long-wavelength leakage, we used a Schott glass OG530
174 placed over the entrance optic being careful to block light paths from the edges that might reach
175 the entrance diffuser optic. The transmission below 460 nm is 0.00001, therefore no light should
176 reach the detectors with the OG530 completely covering the entrance optic. If higher orders of
177 light from the interference filters would reach the detectors, they would begin to be a problem
178 around 600 nm for the 300-nm filter and at longer wavelengths for the other six filters. The
179 nighttime dark readings and 530 Schott blocking filter readings on a clear, sunny day were
180 compared. These readings agreed within the detection limit for the UV-MFRSR.

181
182

183 **Aerosol Optical Depth Retrievals**

184

185 After subtracting the large ozone and Rayleigh optical depth contributions to the total optical
186 depth, a residual remains that is assumed to be aerosol extinction. At Mauna Loa Observatory the
187 aerosol optical depths (AODs) are, in most cases, very small in the visible except in the
188 aftermath of volcanic eruptions (Dutton et al., 1994). The current paper examines AODs in the
189 ultraviolet near 305.6, 311.4, 317.5, 325.1, 332.4, and 367.8 nm where measurements of AOD
190 are infrequently made, especially below 340 nm. These wavelengths are shorter than those
191 measured by most sunphotometers with 340 nm the shortest wavelength measured by
192 AERONET (Holben et al., 2001), for example. Recently, however, López-Solano et al. (2018)
193 used Brewer spectrophotometers to derive AODs at five wavelengths between 306.3 and 320.1
194 nm. They compared AODs measured in this wavelength range by different co-located Brewers
195 and the UVPFR (Carlund et al., 2017). In general, there was excellent agreement between the
196 Brewers and good, but less satisfactory, agreement between Brewers and the UVPFR, however,
197 there was no discussion of the wavelength dependence of the Brewer and UVPFR AODs at these
198 low wavelengths, which we consider next.

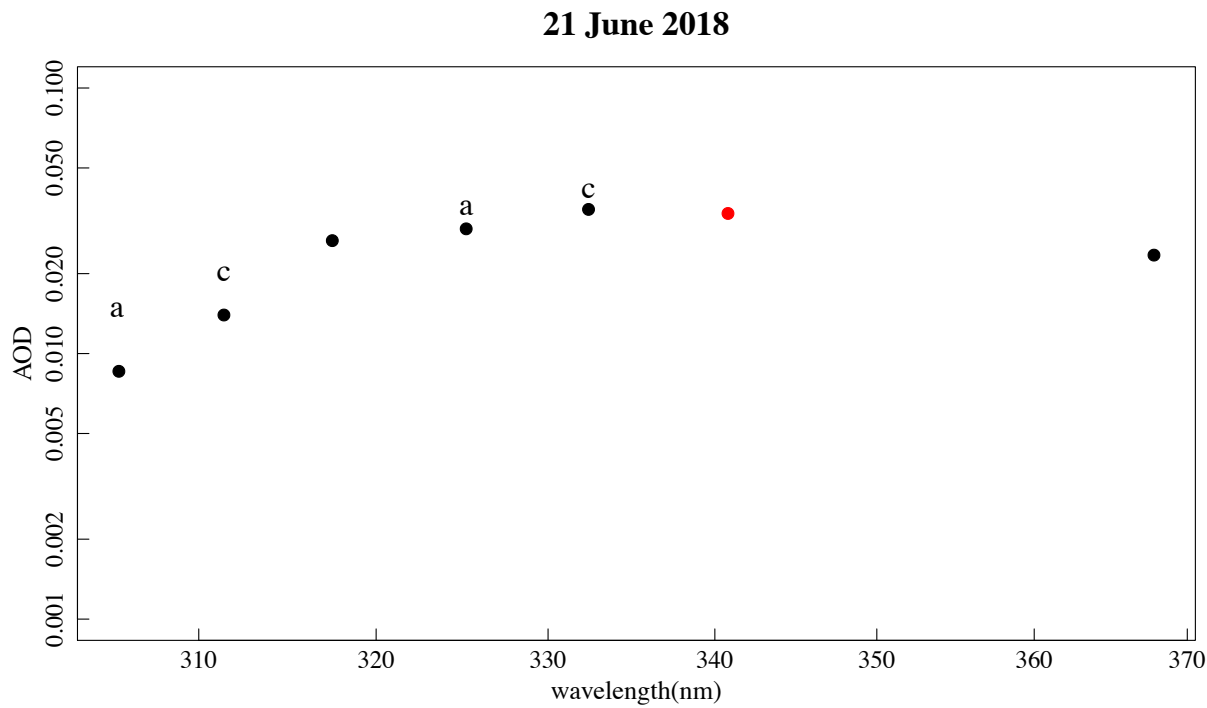
199

200 Figure 4 is typical of the AOD versus wavelength plots from the 43 days of measurements
201 plotted in Fig. 3. *Typical visible* wavelength dependent behavior indicates a negative slope on
202 this type of plot, however, the slope is positive from 305 to 332 nm and then becomes negative
203 after that, with the 368-nm wavelength AOD smaller than the 332-nm wavelength. The red point
204 in Fig. 4 is the average of co-located AERONET data at 340.8 nm (Holben et al., 2001) taken
205 during the same time as the average of the UV-MFRSR data plotted here. This plot indicates
206 consistency between the AERONET and UV-MFRSR data beyond 332 nm. A careful,
207 exhaustive analysis of uncertainties in the UVPFR paper by Carlund et al. (2017) that examines
208 this narrowband filter instrument at the shortest ultraviolet wavelengths close to those of our UV-
209 MFRSR could not explain the similar wavelength dependence (see the right-hand-side of their
210 Fig. 6) that they measured for low aerosol optical depth days in the autumn at Davos,

211 Switzerland. Their Figure 7 supports the argument that the Brewer spectrophotometer
 212 measurements at similar wavelengths should return a similar wavelength dependence. However,
 213 data from Davos in the spring did not show the downturn in AOD at the shortest wavelengths
 214 that the autumn data indicated. In summary, Carlund et al. (2017) suggests that the size of the
 215 uncertainties cannot completely rule out the possibility of a more typical wavelength dependence
 216 with AOD increases with decreasing wavelength.

217
 218 We looked at nitrogen dioxide (NO₂) as a possible contaminant that if not removed could explain
 219 this wavelength behavior, however, the typical amount of NO₂ in the column above Mauna Loa
 220 would necessitate a correction of less than 0.001 optical depths at 332 nm, less at the shorter
 221 wavelengths, and slightly more at 368 nm. When only considering the 332 nm and 368 aerosol
 222 optical depths the plot indicates the typical visible wavelength dependence. Although Fig. 4 is
 223 the only plot of AOD shown, all of the 43 days had similar behavior.

224
 225
 226



227
 228 **Figure 4.** This plot indicates the AOD versus wavelength for the UV-MFRSR filter set at Mauna Loa
 229 Observatory. Instead of a negative slope, this figure, which is typical of the 43 days in this study, indicates a
 230 positive slope with a negative slope indicated only by the two longest wavelengths. The ‘a’ and ‘c’ labels are
 231 included to indicate the wavelength pairs used for the ozone retrievals. The red point is the average of the
 232 AERONET points at 340.8 nm that overlap with the UV-MFRSR averaging period.

233
 234
 235 **Discussion**
 236

237 This paper focuses on data from the Manua Loa Observatory only. It corroborates results
238 reported by Gao et al. (2001) regarding the UV-MFRSR's ability to retrieve ozone column that is
239 in agreement with the Dobson instrument at Mauna Loa Observatory. Figure 3 demonstrates this
240 agreement even though there was no attempt to synchronize ozone observations other than to
241 have them occur on the same day.

242
243 Aerosol optical depths were measured in this very clean environment with expected low values,
244 but an unexpected wavelength dependence. This wavelength dependence is similar to that
245 obtained with an independent, sun-pointed narrowband filter instrument developed and operated
246 at the World Radiation Center (WRC) in Davos, Switzerland. Our and the WRC's attempts to
247 explain this wavelength dependence have yet to yield an understanding of the physics at work
248 here. Systematic biases may be responsible; a better understanding of the very large optical
249 depths associated with ozone absorption and Rayleigh scattering at these wavelengths that have
250 to be subtracted to obtain the small AOD at these wavelengths may require more investigation.
251 On the other hand, further study of environments with somewhat larger aerosol optical depths
252 may indicate that this is, perhaps, associated with aerosol size distributions in some conditions.

253 254 **Appendix**

255
256 After the paper was accepted as a preprint in Atmospheric Measurement Techniques we were
257 contacted by Alexander Smirnov of the AERONET team (aeronet.gsfc.nasa.gov). He made us
258 aware of early Russian papers that measured AODs near the same short UV wavelengths that are
259 plotted in Figure 4. These are discussed in a book by Rozenberg (1966) that was originally
260 published in Russian in 1963, and translated to English for the 1966 publication in the reference
261 list. Figure 97 in the Rozenberg (1996) book is a reproduction of the figure from the paper by
262 Rodionov et al. (1942) that clearly shows AOD decreasing shortward of 380 nm (dubbed by
263 these authors "anomalous transparency"). The observations were made at a high (3 km)
264 mountain site explaining the low AOD values. These authors suggested that a specific aerosol
265 size distribution might explain their wavelength dependence. Rodionov et al.'s (1942)
266 measurements and suggested explanation of them were criticized, but a paper by Sakerin et al.
267 (2000) suggesting that this effect and other unusual spectral dependencies of the AOD could be
268 explained theoretically using specific combinations of nucleation, accumulation, and coarse
269 aerosol modes.

270
271 *Author contributions:* JM drafted the paper and produced the figures. GM produced the data for
272 Fig. 2 and provided details about the Dobson ozone retrievals using the AD and AC pairs.

273
274 *Competing interests.* The contact author has declared that none of the authors has any competing
275 interests.

276
277 *Acknowledgments.* This paper benefited from Dobson ozone retrieval discussions with Peter
278 Effertz and Irina Petropavlovskikh. Kathy Lantz provided the UV-MFRSR data from Mauna Loa
279 Observatory and performed the out-of-band rejection studies. Gary Morris and Kathy Lantz
280 provided a careful reading of the draft paper. Thomas Carlund provided useful insight on WRC's
281 efforts at ultraviolet AOD retrievals using the World Radiation Center (WRC) UV-PFR while he
282 was on sabbatical at the WRC in Davos, Switzerland. Alexander Smirnov was very helpful in

283 pointing out and discussing the earlier papers on Russian measurements and possible
284 explanations for the low UV short wavelength AODs.

285
286 *Financial support.* The publication costs for this paper were covered by the Global Monitoring
287 Laboratory of the National Oceanic and Atmospheric Administration.

288
289

290 **References**

291

292 Bass, A. M. and Paur, R. J. 1985: The ultraviolet cross sections of ozone: I. The measurements.
293 In Atmospheric Ozone - Proceedings of the Quadrennial Ozone Symposium 1984, (Editors: C.S.
294 Zerefos and A. Ghazi), pp. 606-610, Springer, Dordrecht. https://doi.org/10.1007/978-94-009-5313-0_120, 1985.

295

296
297 Bohdaine, B. A., Wood, N. B., Dutton, E. G., Slusser, J. R.: On Rayleigh optical depth
298 calculations. J. Atmos. Ocean. Tech., 16, 1854-1861, [https://doi.org/10.1175/1520-0426\(1999\)016<1854:ORODC>2.0.CO;2](https://doi.org/10.1175/1520-0426(1999)016<1854:ORODC>2.0.CO;2), 1999.

299

300
301 Carlund, T., Kouremeti, N., Kazadzis, S., and Gröbner, J.: Optical depth determination in the UV
302 using a four-channel precision filter radiometer. Atmos. Meas. Tech., 10, 905-923,
303 [doi:10.5194/amt-10-905-2017](https://doi.org/10.5194/amt-10-905-2017), 2017.

304

305 Dutton, E. G., Reddy, P., Ryan, S., and DeLuisi, J. J.: Features and effects of aerosol optical
306 depth observed at Mauna Loa, Hawaii: 1982-1992. J. Geophys. Res., 99, 8295-8306,
307 doi.org/10.1029/93JD03520, 1994.

308

309 Gao, W., Slusser, J., Gibson, J., Scott, G., Bigelow, D., Kerr, J. and McArthur, B.: Direct-Sun
310 column ozone retrieval by the ultraviolet multifilter rotating shadow-band radiometer and
311 comparisons with Brewer and Dobson spectrophotometers. Appl. Optics, 40, 3149-3155, [doi:](https://doi.org/10.1364/AO.40.003149)
312 [10.1364/AO.40.003149](https://doi.org/10.1364/AO.40.003149), 2001.

313

314 Holben, B. N., Tanre, D., Smirnov, A., Eck, T. F., Slutsker, I., Abuhassan, N., Newcomb, W. W.,
315 Schafer, J., Chatenet, B., Lavenue, F., Kaufman, Y. J., Vande Castle, J., Setzer, A., Markham,
316 B., Clark, D., Frouin, R., Halthore, R., Karnieli, A., O'Neill, N. T., Pietras, C., Pinker, R. T.,
317 Voss, K., and Zibordi, G.: An emerging ground-based aerosol climatology: Aerosol optical depth
318 from AERONET, J. Geophys. Res., 106, 12067-12097, <https://doi.org/10.1029/2001JD900014>,
319 2001.

320

321 Komhyr, W. D. Operations Handbook—Ozone Observations with a Dobson Spectrophotometer,
322 rev., Evans, R. D., AW No. 183, WMO/TD -No. 1469, 2008.

323

324 López-Solano, J., Redondas, A., Carlund, T., Rodriguez-Franco, J. J., Diémoz, H., León-Luis, S.
325 F., Hernández-Cruz, B., Guirado-Fuentes, C., Kouremeti, N., Gröbner, J., Kazadzis, S., Carreño,
326 V., Berjón, A., Santana-Díaz, D., Rodríguez-Valido, M., De Bock, V., Moreta, J. R., Rimmer, J.,
327 Smedley, A. R. D., Boulkelia, L., Jepsen, N., Eriksen, P., Bais, A. F., Shiroto, V., Vilaplana, J.

328 M., Wilson, K. M., and Karppinen, T.: Aerosol optical depth in the European Brewer Network,
329 Atmos. Chem. Phys., 18, 3885–3902, <https://doi.org/10.5194/acp-18-3885-2018>, 2018.
330
331 Michalsky, J., Denn, F., Flynn, C., Hodges, G., Kiedron, P. Koontz, A., Schlemmer, J., and
332 Schwartz, S. E.: Climatology of aerosol optical depth in north-central Oklahoma: 1992:2008, J.
333 Geophys. Res., D07203, <https://doi.org/10.1029/2009JD012197>, 2010.
334
335 Michalsky, J., Schlemmer, J., Berkheiser III, W., Berndt, J., Harrison, L., Laulainen, N., Larson,
336 N., and Barnard, J.: Multi-year measurements of aerosol optical depth in the Atmospheric
337 Radiation Measurement and Quantitative Links programs, J. Geophys. Res., 106, 12099-12107,
338 <https://doi.org/10.1029/2001JD900096>, 2001.
339
340 Rozenberg, G.V.: Twilight: A Study in Atmospheric Optics, Plenum Press, New York, 358 pp.,
341 ISBN 0608129313, 9780608129310, 1996. (Originally published in Moscow by State Press for
342 Physico Mathematical Literature 1963.)
343
344 Rodionov, S. F., Pavlova, E. N., Rduktovshaya, E. V. and Reinov, N. T.: Izv. Nauk SSSR, Ser.
345 Geogr. Geofiz., 6, No. 4, 135 (1942).
346
347 Sakerin, S. M., Rakhimov, R. F., Makienko, E. V., and Kabanov, D. M.: Interpretation of the
348 anomalous spectral dependence of the aerosol optical depth in the atmosphere. Part 1. Formal
349 analysis of situation, Atmos. Oceanic Opt, 13, No. 9, 754-758, 2000.
350
351 Staehelin, J., Kerr, J., Evans, R. and Vanicek, K., Comparison of total ozone measurements of
352 Dobson and Brewer spectrophotometers and recommended transfer functions, WMO/GAW 149
353 (WMO TD 1147), 39 pp., 2003.